Can Doping Graphite Trigger Room Temperature Superconductivity? Evidence for Granular High-Temperature Superconductivity in Water-Treated Graphite Powder

T. Scheike, W. Böhlmann, P. Esquinazi, J. Barzola-Quiquia, A. Ballestar, and A. Setzer*

The existence of room-temperature superconductivity (RTS) was claimed in 1974 through the observation of Josephson tunneling behavior of the electric current in response to a magnetic field applied to aluminum-carbon-aluminum sandwiches.[1] In that work, the carbon layer consisted of small, strongly distorted graphite crystallites. Magnetization measurements conducted twenty six years later also provided evidence for the existence of RTS in parts of oriented graphite samples.[2] Similar claims were subsequently published for, for example, an n-type diamond surface[3] as well as for palladium hydride.[4] None of those reported results, however, was later independently verified, such that the existence of RTS remains an apparently unreachable dream in science. The possibility to have high-temperature superconductivity in graphite,[5] at its interfaces,[6] as well as in disordered carbon[7] has been the subject of only a few experimental studies but of a large number of theoretical works in the last 10 years. For example, one expects to find this phenomenon either by doping graphene layers,[8–11] at the graphite surface region due to a topologically protected flat band[12] or in disordered graphite regions;[13] *p*-wave[13] as well as *d*-wave superconductivity[14,11] were predicted. Trying to dope graphite flakes, we found that the magnetization of pure, graphite powder, with a grain size of several tens of micrometers, after a simple treatment with pure water shows clear and reproducible granular superconducting behavior with a critical temperature above 300 K. The observed magnetic characteristics as a function of temperature, magnetic field and time, provide evidence for weakly coupled grains through Josephson interactions, revealing the existence of superconducting vortices.

For the preparation of the water-treated graphite powder, 100 mg of ultra pure graphite powder was mixed (see the Experimental Section) into 20 mL distilled water and this mixture is continuously stirred at room temperature. At the beginning of the preparation the graphite grains floated on the surface of the water because of their high hydrophobicity. After ≈1 h, one can observe that the graphite powder forms a homogenous, aqueous suspension. After further stirring for 22 h, the obtained powder was recovered by filtration with a clean nonmetallic filter and dried at 100 °C overnight. The same procedure was repeated several times and checked for the reproducibility of the measured properties. Without exception, all prepared samples with the same powder showed superconducting behavior, provided the powder were not pressed into compact pellets.

The first high-temperature superconducting (HTSC) oxide samples showed typical signs for granular superconductivity, an issue very well described in the literature of the late 1980s and 1990s. In a granular superconductor in which a minor part of the sample shows superconductivity, the magnetic field-induced hysteresis (in field (H) and temperature (T) is the tool one uses to provide evidence for superconductivity and the existence of Abrikosov and/or Josephson vortices (fluxons). Measurement of the hysteresis between the magnetic moment $m(T)$ in the zero-field cooled (ZFC) and field cooled (FC) states is a method that does not require any background subtraction and it is relatively free from artifacts from the superconducting quantum interferometer device (SQUID).[15]

We present first the results for the untreated graphite powder. In **Figure 1**a the total diamagnetic signal at 300 K (right y-axis) and the small hysteresis loop obtained after subtraction of the linear diamagnetic background is shown. This field hysteresis loop of the magnetization with a remanence $M(H = 0) \approx 8 \times 10^{-6}$ emu/g after sweeping to the maximum field $H_{max} = 400$ Oe is about one order of magnitude smaller than the one obtained for the water treated powder at the same experimental conditions. Figure 1b shows the temperature dependence of the magnetic moment $m(T)$ of the same untreated powder in the ZFC and FC states at $H = 500$ Oe. There is a negligible temperature hysteresis (with a reproducibility of 0.3 μemu) in most of the temperature range (see Figure 1c). We will see below that the water treatment enhances drastically both hysteresis beyond experimental errors.

Figure 2a shows $m(T)$ for the water-treated powder in the ZFC and FC states at $H = 500$ Oe. The hysteresis is clearly observable and indicates the presence of pinned magnetic entities in the sample. Since magnetic order can be triggered in graphite by introducing defects (or hydrogen[16]) or after chemical treatment,[17] it is necessary to clarify whether the observed behavior is due to a ferromagnetic signal. To answer this, we conducted the same kind of measurement at different applied field strengths. The results of the difference between the magnetic

T. Scheike, Dr. W. Böhlmann, Prof. P. Esquinazi, Dr. J. Barzola-Quiquia, A. Ballestar, A. Setzer
Division of Superconductivity and Magnetism
Institut für Experimentelle Physik II
Fakultät für Physik und Geowissenschaften der Universität Leipzig, Linnéstrasse 5
D-04103 Leipzig, Germany
E-mail: esquin@physik.uni-leipzig.de

DOI: 10.1002/adma.201202219

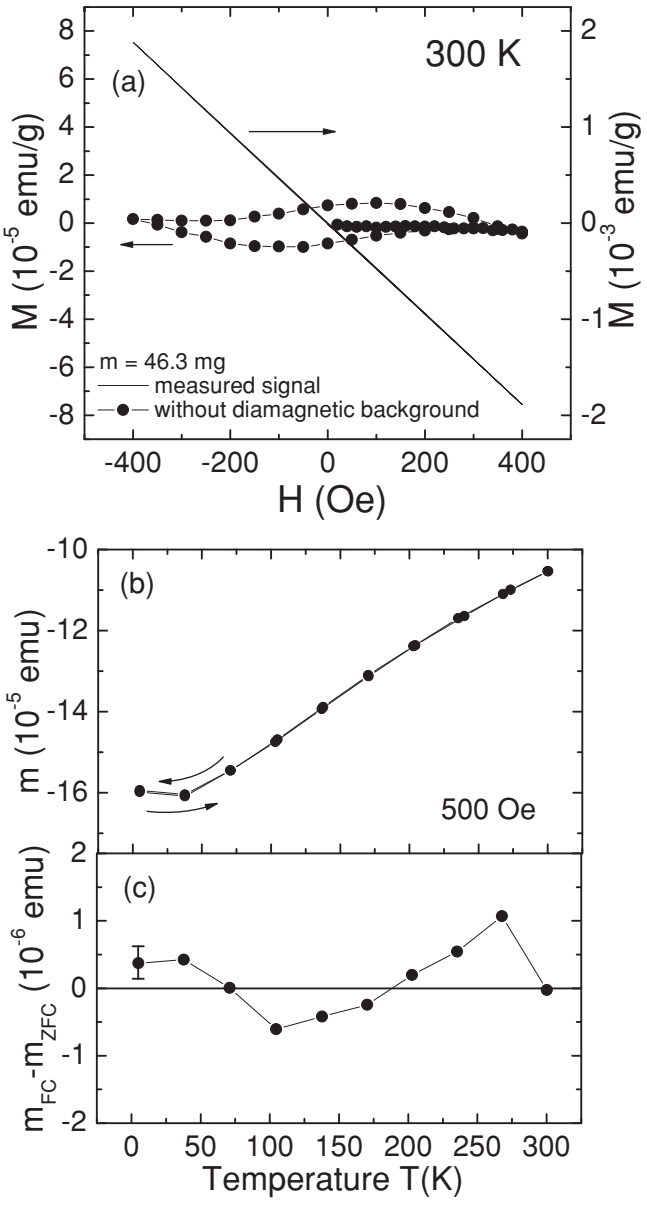

Figure 1. a) Magnetic moment at 300 K measured for the untreated (nonpressed) graphite powder (right *y*-axis) as a function of the applied field. Left *y*-axis: the same data after subtraction of the diamagnetic linear background. b) Magnetic moment without any subtraction as a function of temperature in the ZFC (lower curve) and FC states at 500 Oe of the same untreated graphite powder. c) Temperature dependence of the difference between the upper FC and ZFC curves for a 500 Oe applied field.

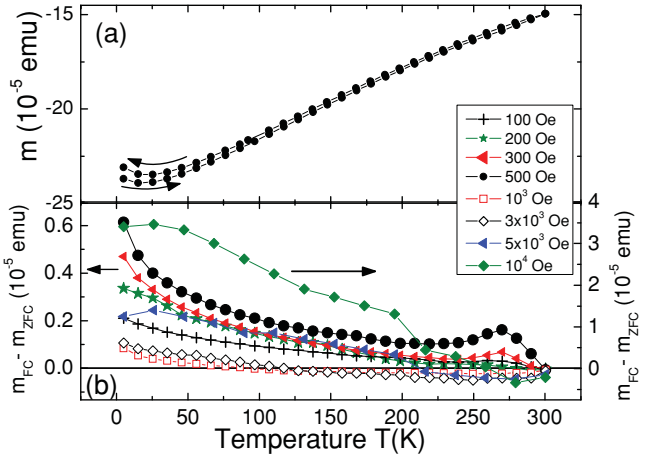

Figure 2. a) Magnetic moment, without any subtraction, as a function of temperature in the ZFC (lower curve) and FC states at 500 Oe of the water-treated graphite powder. (b) Temperature dependence of the difference between the upper FC and ZFC curves at different applied field strengths. Left y-axis corresponds to applied fields up to 500 Oe; right y-axis corresponds to higher applied fields. The results were obtained for a nonpressed water treated graphite powder sample of mass, m = 61.5 mg.

moment in the ZFC and FC states, $\Delta m(T) = m_{FC}(T) - m_{ZFC}(T)$ and at different applied fields are shown in Figure 2b. At applied field strengths of $H \leq 500$ Oe, $\Delta m(T)$ increases with the field strength at all temperatures. However, at applied field strengths of $H = 10^3$ Oe and 3×10^3 Oe, $\Delta m(T)$ is nearly the same showing a weak *T*-dependence with a crossing point, T_i, from small negative to positive values below ≈120 K, see Figure 2b. At $H \geq 5 \times 10^3$ Oe, $\Delta m(T)$ increases again with the field strength at $T < T_i$.

We note that the T_i shifts to higher *T* when stronger fields are applied.[15] The observed behavior is neither compatible with the pinning of magnetic domain walls in general nor with the ferromagnetic behavior of graphite powder;[17] however, it is compatible with granular superconductivity. To describe the observed behavior, we used below well-known concepts of superconducting phenomena. We note, however, that at this stage and due to the observed behavior, we cannot rule that a more sophisticated explanation is appropriate as would be the case for an unconventional pairing mechanism.

We assume that part of the powder is superconducting and that under a magnetic field, a superconducting loop can be produced through the grains, which are coupled by intergrain Josephson links. The low field response of this system can be understood by the single junction superconducting quantum interferometer model.[18–21] Two Josephson critical fields can be defined,[18] namely, h_{c1}^J, i.e., the lower Josephson critical field as the characteristic field above which fluxons penetrate into the sample, and h_{c2}^J, the Josephson decoupling field above which the superconducting grains' response is the same as that of isolated superconducting grains. At a maximum applied field strength, $H_{max} < h_{c1}^J$, no hysteresis or remanence is observed and the magnetization is given by the macroscopic shielding currents (running through the weakly coupled grains) and the microscopic current loops (circulating around the grains) within their corresponding penetration depths. This nonhysteretic, reversible region can be recognized by measuring the remanent loop width at zero field $\Delta m(H = 0) = m_H+(H = 0) - m_H-(H = 0)$ as a function of H_{max} at different constant temperatures (see **Figure 3**). Here, $m_H+,-$ are the remanent magnetic moments after returning to the $H = 0$ state from $+H_{max}$ or $-H_{max}$. We note that the overall behavior of $\Delta m(H = 0, H_{max}, T)$ is very similar to that observed in granular[19–21] as well as in single crystalline[22] HTSC oxides. From these results, and as described

Adv. Mater. **2012**,
DOI: 10.1002/adma.201202219

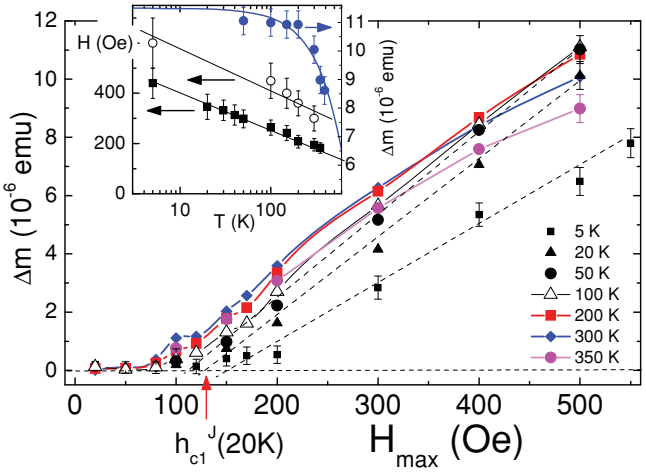

Figure 3. Full remanent ($H = 0$) magnetic moment width Δm of the hysteresis loops measured after cycling the sample (61.5 mg) to a maximum field strength, H_{max}, at different temperatures. The lower Josephson critical field, h_{c1}^J, is defined at the crossing point between the zero line and the linear increasing lines (dashed straight lines as examples for 5, 20, and 50 K). Similar values and temperature dependence are obtained by plotting the data semilogarithmically and defining h_{c1}^J at constant $\Delta m = 3 \times 10^{-7}$ emu. The red arrow shows this field for the curve measured at 20 K. Inset: temperature dependence of the lower (close squares) and upper (open circles) critical Josephson fields (left y-axis). The measured values of the lower critical field were multiplied by a factor of three in this figure. The right y-axis corresponds to the width, Δm, of the hysteresis field loop at zero field after cycling the field to $H_{max} = 500$ Oe. The blue curve follows $\Delta m(T) = 11.5$ [μemu] $(1-(T/1050\ [K])^{1.5})$.

in Figure 3, we determine $h_{c1}^J(T)$. The obtained $h_{c1}^J(T)$ values are not only one to two orders of magnitude larger than those obtained in granular HTSC oxides[19–21] but they follow an unusual –log T dependence (see inset in Figure 3) with an apparent critical temperature $T_c > 10^3$ K, defined at $h_{c1}^J(T_c) \rightarrow 0$ Oe after a linear extrapolation. At $h_{c1}^J < H_{max} < h_{c2}^J$, intergranular and London currents around the grains can trap fluxons as well as intragranular Abrikosov vortices (produced by the displacement of the first ones[23]) in an irreversible manner producing hysteresis in the temperature loops, as shown in Figure 2, as well as field hysteresis and a finite loop width $\Delta m(H = 0)$, see **Figure 4**.

Figure 4 shows the field hysteresis loops after subtraction of the linear diamagnetic background (for a given temperature) measured at different H_{max} at 5 K (a) and 300 K (b). For $h_{c1}^J(T) < H_{max} < h_{c2}^J(T)$ and, as expected[18,19], the overall shape of the hysteresis loops resembles the one obtained using the Bean model for bulk superconductors.[24] As example, we compare in Figure 4a the loop at 5 K and $H_{max} = 400$ Oe with the one calculated using the Bean model with a full penetration field $H_p = 270$ Oe. At high enough H_{max}, however, a change of the slope of the virgin curve $m(H)$ and an anomalous shrinking of the hysteresis width (instead of a saturation) are measured, see Figures 4a,b. This behavior has been observed also in granular HTSC oxides and it is well understood assuming that at $H_{max} > h_{c2}^J(T)$, but smaller than the lower intragrain critical field H_{c1}, there is a transition to a nonhysteretic mode and the

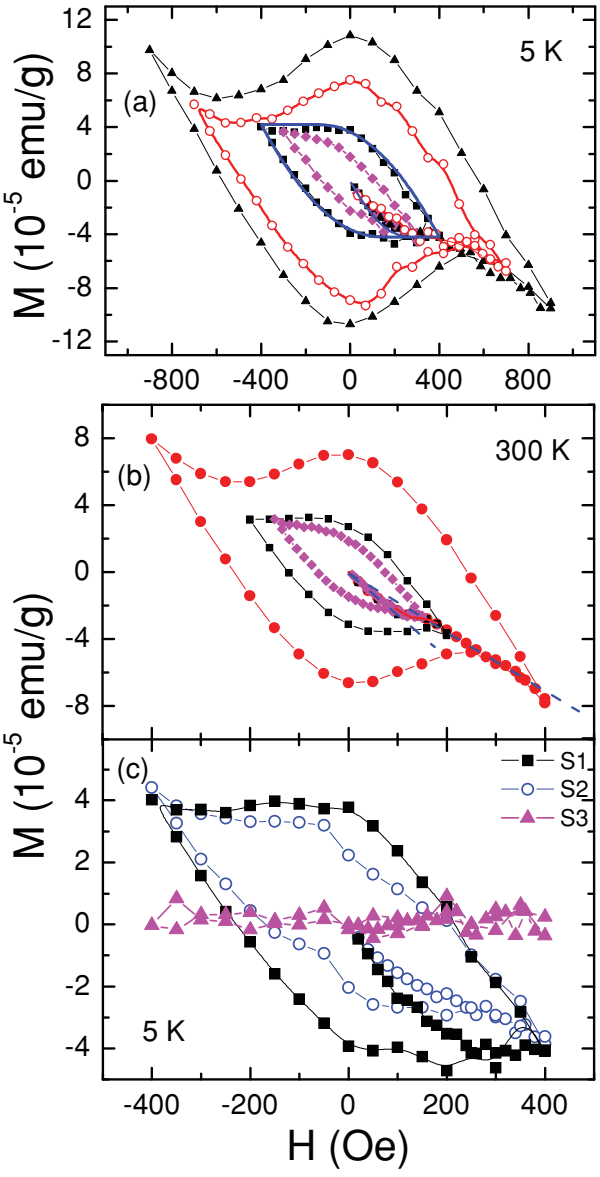

Figure 4. a) Magnetization field hysteresis loops at different maximum field strengths: H_{max} (300, 400, 700, and 900 Oe) and at 5 K. The magnetization was calculated dividing the magnetic moment by the total sample mass. The blue continuous curve that fits the loop measured for $H_{max} = 400$ Oe was calculated with the Bean model[24] with a penetration field of $H_p = 270$ Oe. A linear diamagnetic background -6.8×10^{-6} H (Oe) emu/g was subtracted from the data. b) The same as (a) but at 300 K and for $H_{max} = 150$, 200, and 400 Oe. The two dashed lines are a guide to the eye that highlight the change of the slope when the field is increased from $H << h_{c2}^J$ to $H > h_{c2}^J$. A linear diamagnetic background of -4.6×10^{-6} H(Oe) emu/g was subtracted from the data. c) Hysteresis loops at 5 K and for $H_{max} = 400$ Oe for the water treated powder (S1, mass = 61.5 mg), the same powder but after pressing it in a pellet with a pressure of 18 ± 5 MPa (S2, mass = 33.6 mg) and after pressing it with a pressure of 60 ± 20 MPa (S3, mass = 33.7 mg). The corresponding diamagnetic linear backgrounds were subtracted from the measured data. As shown, for example, in Ref.[2], the raw data have the sum of the two contributions, from the diamagnetic and superconducting regions. For example, from the results in (a), there is a ratio between the remanence to the non-superconducting diamagnetic contribution at 100 Oe of ≈0.15 and at 10^3 Oe of ≈0.015. Note the difference in the field x-scale between (a) and (b,c).

magnetic moment in this field range is due to the flux expulsion from the isolated superconducting grains.[19,20] Defining $h_{c2}^J(T)$ at the beginning of the linear reversible region at high fields, we obtained the values shown in the inset of Figure 3. The obtained $h_{c2}^J(T)$ shows a similar T-dependence to $h_{c1}^J(T)$, leading to a constant ratio in the measured temperature range $h_{c2}^J(T)/h_{c1}^J(T) = 4 \pm 0.5$, similar to values obtained in granular HTSC and in agreement with model predictions in terms of weakly coupled superconducting grains.[20] According to this model, the obtained values of the Josephson critical fields suggest much larger Josephson critical currents for similar loop parameters than in the HTSC.

A rough estimate of the relative superconducting mass in our samples gives ≈100 ppm, taking the diamagnetic slope at low fields without any demagnetization factor. Although small, this superconducting yield is of relevance and, interestingly, of the same order as the ferromagnetic one triggered in graphite by chemical methods.[17] With this mass we can estimate the superconducting magnetization and through this, some parameters of the superconducting granular system. From the total magnetization width obtained at $H = 0$ Oe and at $T = 5$ K ($H_{max} = 400$ Oe), following the Bean model, we estimate a critical intergranular Josephson current density of 10^{11} A/m$^2 > J_c \approx \Delta M/a > 10^{10}$ A/m^2 for 1 μm < a < 10 μm, where a is the corresponding effective grain length. For the same range of a and with the lower Josephson critical field strength (see Figure 3) of $h_{c1}^J(5\text{ K}) \approx 150$ Oe $\approx J_c\lambda_J$ we get a Josephson penetration depth of 0.1 μm < λ_J(5 K) < 1 μm, i.e., an order of magnitude smaller than the corresponding length.

The non-monotonic behavior with field obtained for $\Delta m\ (T) = m_{FC}(T) - m_{ZFC}(T)$ shown in Figure 2b, is compatible with the description provided above. Some further details are worth mentioning. The maximum in $\Delta m\ (T)$ observed at high temperatures near the turning temperature of 300 K at $H \leq 500$ Oe, appears to be related to the so-called peak effect in granular superconductors originated by the change of the pinning regime between fluxons and Abrikosov vortices.[23] Above 600 Oe, i.e., above the corresponding $h_{c2}^J(T)$ when the Josephson coupling between the grains is destroyed, this peak vanishes and $\Delta m(T)$ decreases to nearly T-independent (small negative) values. $\Delta m(T)$ changes to positive below T_i, which occurs when $H < h_{c2}^J(T)$. At applied fields $H > 3000$ Oe, $\Delta m(T)$ increases again suggesting that the pinning of intragranular Abrikosov vortices in the decoupled grains starts to play a role. These results indicate that the effective lower intragrain critical field, H_{c1}, is also very high. Note that $\Delta m(T)$ increases steadily with the field strength[15] above some threshold suggesting that the pinning increases with field strength up to the highest measured temperature. This pinning increase with field strength is, in principle, commonly seen in superconductors, albeit at field strengths much lower than the upper critical value of $H_{c2}(T)$.

Because of the finite vortex pinning strength, we expect to measure a time relaxation of the magnetic moment after reaching a field strength from a different, previously prepared field state in the sample. This well known flux creep phenomenon shows a logarithmic time dependence of the form $m(t)/m(0) = 1 - m_1 \ln(1 + t/\tau_0)$, $m_1 \approx k_B T/U_a$, where U_a is an apparent flux creep activation energy and τ_0 is a time constant that determines a transient stage before the beginning of the logarithmic relaxation.[25] The time dependence of the magnetic moment shown in **Figure 5** was obtained at each temperature after cycling the field to 300 Oe and then decreasing it to the remanent state ($H = 0$). The observed dependence can be very well described by the above logarithmic time function. From the fitted values obtained at high temperatures, we obtain $U_a \approx 8000$ K. This high activation energy value (at H = 0 Oe) would mean that the thermally activated vortex or fluxon diffusion would affect the critical current density mainly at high enough temperatures. The measured temperature dependence of the remanent full hysteresis width $\Delta m(H_{max} = 500$ Oe, $H = 0)(T) \propto J_c(T, H = 0)$ shown in the inset of Figure 3 agrees with this expectation. We note also that the influence of flux creep is one possible reason for the (small) negative and not strictly zero values of $\Delta m(T) = m_{FC}(T) - m_{ZFC}(T)$ at high enough temperatures and field strengths shown in Figure 2b. The time relaxation at much higher fields is strongly reduced, also suggesting an increase of U_a with applied field strength. As an example, we show in the inset of Figure 5 the time relaxation for the same sample at a field strength of 10^4 Oe coming from a stationary state at a field strength of 2×10^4 Oe at 5 and 300 K. The relative change with time at this field strength drastically decreased to values intrinsic to the system, i.e., the observed time decay is sample independent as well as sample-temperature independent (see Figure 5).

The described treatment of the graphite powder with water leads to changes of the magnetic properties as shown above. It is possible that the water molecules form a uniform structured layer at the graphite/water interface, as has been reported previously.[26] Increasing the water treatment time,

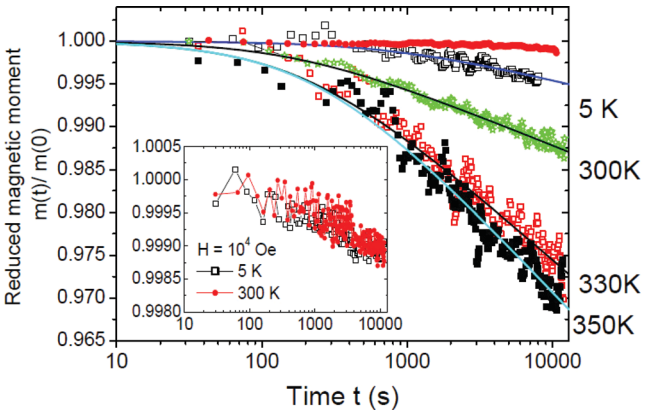

Figure 5. Time dependence of the normalized remanent ($H = 0$) magnetic moment at different fixed temperatures of a water treated powder of mass = 61.5 mg. Initially, a field of 300 Oe was applied to the sample and afterwards it was decreased to a nominally zero field strength. The continuous lines are fits to the function $m(t)/m(0) = 1 - m_1 \ln(1 + (t/\tau_0))$ with m_1 and τ_0 free parameters (for $T = 5$, 300, 330, and 350 K, the fitting parameters and their confidence errors are (m_1, τ_0): $(1.8 \pm 0.6)\ 10^{-3}$, (400 ± 200) s; $(3 \pm 0.5)\ 10^{-3}$, (170 ± 80) s; $(7 \pm 0.5)\ 10^{-3}$, (250 ± 80) s; $(9 \pm 0.5)\ 10^{-3}$, (300 ± 100) s. To check for possible SQUID-related artifacts in the time relaxation the red close circles (upper curve) correspond to the results obtained after a similar procedure at 300 K for a Dy_2O_3 sample, which had a similar absolute magnetic moment as the graphite powder sample. Inset: similar data obtained at 5 and 300 K but at a field strength of 10^4 Oe coming from a state of 2×10^4 Oe.

Adv. Mater. 2012,
DOI: 10.1002/adma.201202219

the hydrophobicity of the graphite grains is reduced leading to chemisorption driven by a chemical reaction at the exposed surfaces.[27] Which kind of structure or stoichiometry the superconducting graphite part has and whether the superconductivity appears at graphite interfaces (or sandwiches) produced after the water-treated graphite grains clamp together, remains an issue to be clarified in future studies. It may be that water treatment dopes parts of the grain surfaces with hydrogen and this element plays an important role, as has been observed with respect to the magnetic order found in graphite.[16,17] To check this, we have exposed the virgin graphite powder to hydrogen plasma for 75 min at room temperature. The prepared powder shows the same characteristics as the water treated one[15] indicating that hydrogen may play a role in this phenomenon. Whether water, hydrogen or oxygen molecules can enter into the graphite lattice and trigger superconductivity, similar to the apparent intercalation processes and superconductivity found in $FeTe_{1-x}S_x$ samples after their treatment with hot alcoholic beverages,[28] remains an interesting question to be answered in future studies. Furthermore, the superconducting signals decrease after annealing the water-treated powder in vacuum.[15]

With respect to the study of Antonowicz,[1] we believe that the results of this study were correct and that the reported metastability with time and the weak reproducibility of the phenomenon relates to the state of the interfaces or junctions between the graphite grains, as well as to a macroscopic size effect when the effective radius of several coupled grains increases. The larger the size of the macroscopic superconducting loop radius R, the smaller the critical current density, i.e., $J_c \propto 1/R$ as observed in granular HTSC.[19] In our water treated powder samples this might be achieved just by pressing them. To check this we have pressed the previously treated and measured graphite powder into pellets with two different pressures. As shown in Figure 4c, the width of the superconducting hysteresis loop decreases by ≈40% at $H = 0$ after compacting the powder (S1) with a pressure of ≈18 MPa. For a pellet prepared with a three times larger pressure using the same treated powder (S1), the superconducting-like hysteresis loop vanishes completely, see Figure 4c. Clearly, the vanishing of the superconducting signals by pressing the treated powder and the low yield obtained by our water treatment strongly limit the use of direct electrical transport measurements of such pellets to check for superconducting signals by transport. Instead, transport measurements in micrometer-sized grains are needed. Although these measurements have not yet been conducted in water treated grains, it is worth mentioning the transport results obtained in micrometer-sized graphite lamellae with a large density of two-dimensional interfaces.[6] The high carrier density found at these interfaces[29] (due to the influence of hydrogen, lattice defects and/or a different graphite stacking) as well as several other experimental hints,[6] suggest that granular superconductivity exist at those interfaces. The obtained I-V characteristic curves as well as the SQUID results obtained for this kind of sample provide evidence for granular superconductivity above 100 K.[15] In this case one may ask whether finite fluxon pinning can exist in a superconducting, two dimensional interface. Avoiding here any speculation about the origin of pinning and any possible coupling mechanism necessary to trigger superconductivity at the interfaces, we note that magnetization hysteresis loops have been already observed in Bi bicrystals as well as in Bi_xSb_{1-x} bi- and trycrystals where superconductivity has been proved to exist at interfaces.[30]

The origin of the observed RTS and the overall behavior, especially of the large values and the logarithmic T-dependence of the Josephson critical fields and the large critical temperature are clearly unconventional. Taking into account that atomic lattice defects as well as hydrogen can be also a source of magnetic order in the graphite structure, future studies should clarify its correlation to RTS. If there is such correlation, we note that since p-type superconductivity was predicted for graphite,[13] it should have a strong influence on the fluxon pinning strength and, in turn, on the superconducting response.[31] The observed increase of the irreversible behavior can be ascribed to an increase in vortex pinning at field strengths above a certain threshold. Whether this increase is due to the very high $H_{c2}(T)$ values or if it is related to the type of the order parameter should be clarified in the future. Finally, we would like to note that although the superconducting yield with our treatment is small, and its phase and stoichiometry remain to be determined, the overall results indicate that room temperature superconductivity appears to be attainable, and that the methods used here may pave the way for a new generation of superconducting devices with unexpected benefits for society.

Experimental Section

Ultrapure graphite powder RWA/T from SGL Carbon GmbH (Werk Ringsdorff, Germany) was used. The measured impurities by particle induced X-ray emission (PIXE) in µg/g were: Al < 11, P < 3.6, S < 2.2, Cl < 1.4, K < 0.75, Ca < 0.53, Ti < 0.29, V < 0.28, Cr < 0.24, Fe < 0.19, Ni < 0.17, Cu < 0.2 and Zn< 0.31. After the water treatment, the elemental analysis of the powder showed a slight increase in the oxygen concentration from 1.85 to 2.15 at%. It is likely that the hydrogen concentration also increased after treatment. The powder in the virgin, as-received state and after water treatment was packed in polymer foils of less than 1 mg mass, the magnetic background signal of which (measured independently) was negligible in all measurements. The pressed powder (pellets) were prepared using a pressure cell avoiding any contact of the powder with metallic surfaces.

The magnetic measurements were conducted with a SQUID magnetometer from Quantum Design. Because the critical temperature of the superconducting powder appears to be unreachable with the available techniques, a "zero vortex" virgin state is not really achieved. A near zero vortex state can be obtained by cycling the field to zero using the oscillating mode of the SQUID system. Field hysteresis loops at field $H_{max} > 1000$ Oe are certainly possible but the superconducting solenoid used by the SQUID system shows a hysteresis that influences the measured magnetic moment and must be subtracted from the data in a nonsimple and transparent way. An example for this high field hysteresis due to the solenoid (or other SQUID artifact) can be seen in Ref.[15] This is the reason why only hysteresis loops measured at lower fields are presented. We note that this artifact is negligible in the ZFC-FC hysteresis measurements.

Supporting Information

Supporting Information is available from the Wiley Online Library or from the author.

Acknowledgements

This research is supported by the Deutsche Forschungsgemeinschaft under Contract No. DFG ES 86/16-1. A.B. was supported by the project ESF-Nano under the Graduate School of Natural Sciences "BuildMona".

Received: June 2, 2012
Revised: July 16, 2012
Published online:

[1] K. Antonowicz, *Nature* **1974**, *247*, 358–360.
[2] Y. Kopelevich, P. Esquinazi, J. H. S. Torres, S. Moehlecke, *J. Low Temp. Phys.* **2000**, *119*, 691–702.
[3] J. F. Prins, *Semicond. Sci. Technol.* **2003**, *18*, S131–S140.
[4] P. Tripodi, D. Di Gioacchino, R. Borelli, J. D. Vinko, *Physica C: Superconductivity* **2003**, *388–389*, 571 – 572.
[5] Y. Kopelevich, P. Esquinazi, *J. Low Temp. Phys.* **2007**, *146*, 629–639.
[6] a) J. Barzola-Quiquia, A. Ballestar, S. Dusari, P. Esquinazi, Experimental Study of the Intrinsic and Extrinsic Transport Properties of Graphite and Multigraphene Samples, in *Graphene* (Ed: J. R. Gong), Intech, Open Access Publisher **2011**, Chap. 8; b) A. Ballestar, J. Barzola-Quiquia, P. Esquinazi, arXiv:1206.2463.
[7] I. Felner, Y. Kopelevich, *Phys. Rev. B* **2009**, *79*, 233409.
[8] B. Uchoa, A. H. Castro Neto, *Phys. Rev. Lett.* **2007**, *98*, 146801.
[9] S. Pathak, V. B. Shenoy, G. Baskaran, *Phys. Rev. B* **2010**, *81*, 085431.
[10] G. Profeta, M. Calandra, F. Mauri, *Nat. Phys.* **2012**, *8*, 131–134.
[11] R. Nandkishore, L. S. Levitov, A. V. Chubukov, *Nat. Phys.* **2012**, *8*, 158–163.
[12] N. B. Kopnin, T. T. Heikkilä, G. E. Volovik, *Phys. Rev. B* **2011**, *83*, 220503.
[13] J. Gonzalez, F. Guinea, M. A. H. Vozmediano, *Phys. Rev. B* **2001**, *63*, 134421.
[14] A. M. Black-Schaffer, S. Doniach, *Phys. Rev. B* **2007**, *75*, 134512.
[15] For further experimental results see the Supporting Information.
[16] H. Ohldag, P. Esquinazi, E. Arenholz, D. Spemann, M. Rothermel, A. Setzer, T. Butz, *New J. Phys.* **2010**, *12*, 123012.
[17] J. Barzola-Quiquia, W. Böhlmann, P. Esquinazi, A. Schadewitz, A. Ballestar, S. Dusari, L. Schultze-Nobre, B. Kersting, *Appl. Phys. Lett.* **2011**, *98*, 192511.
[18] J. R. Clem, *Physica C* **1988**, *153–155*, 50–55.
[19] S. Senoussi, C. Aguillon, S. Hadjoudj, *Physica C* **1991**, *175*, 215–225.
[20] M. Borik, M. Chernikov, V. Veselago, V. Stepankin, *J. Low Temp. Phys.* **1991**, *85*, 283–294.
[21] B. Andrzejewski, E. Guilmeau, Ch. Simon, *Supercond. Sci. Technol.* **2001**, *14*, 904–909.
[22] M. W. McElfresh, Y. Yeshurun, A. P. Malozemoff, F. Holtzberg, *Physica A* **1990**, *168*, 308–318.
[23] V. K. Ignatjev, *Low Temp. Phys.* **1998**, *24*, 339–344.
[24] C. P. Bean, *Rev. Mod. Phys.* **1964**, *36*, 31–39.
[25] A. Gurevich, H. Küpfer, *Phys. Rev. B* **1993**, *48*, 6477–6487.
[26] K. Suzuki, N. Oyabu, K. Kobayashi, K. Matsushige, H. Yamada, *Appl. Phys. Express* **2011**, *4*, 125102.
[27] K. Oura, V. G. Lifshits, A. A. Saranin, A. V. Zotov, M. Katayama, *Surface Science, An Introduction,* Springer, Berlin **2003**.
[28] K. Deguchi, Y. Mizuguchi, Y. Kawasaki, T. Ozaki, S. Tsuda, T. Yamaguchi, Y. Takano, *Supercond. Sci. Technol.* **2011**, *24*, 055008.
[29] N. García, P. Esquinazi, J. Barzola-Quiquia, S. Dusari, *New J. Phys.* **2012**, *14*, 053015.
[30] a) F. M. Muntyanu, A. Gilewski, K. Nenkov, A. J. Zaleski, V. Chistol, *Phys. Rev. B* **2007**, *76*, 014532; b) F. M. Muntyanu, A. Gilewski, K. Nenkov, A. J. Zaleski, V. Chistol, *Phys. Status Solidi B* **2011**, *248*, 2903.
[31] M. Sigrist, *Physica B* **2000**, *280*, 154–158.